

Determination of optical parameters in quasi-monochromatic LEDs for implementation of lighting systems with tunable correlated color temperature

D.V. Pekur¹, V.M. Sorokin¹, Yu.E. Nikolaenko², I.V. Pekur¹, M.A. Minyaylo¹

¹V. Lashkaryov Institute of Semiconductor Physics, National Academy of Sciences of Ukraine
41, prosp. Nauky, 03680 Kyiv, Ukraine,

E-mail: demid.pekur@gmail.com, vsorokin@isp.kiev.ua

²National Technical University of Ukraine "Igor Sikorsky Kyiv Polytechnic Institute"

37, prosp. Peremohy, 03056 Kyiv, Ukraine,

E-mail: y.nikolaenko@kpi.ua

Abstract. The paper proposes a new method for determining the optimal peak wavelengths of quasi-monochromatic LEDs, when they are combined with white broadband high-power LEDs in lighting systems with tunable correlated color temperature (CCT). Simulation of the resulting radiation spectrum was used to demonstrate the possibility to use the developed method in LED lighting systems with tunable parameters of the synthesized light. The study enables to determine the peak wavelengths of quasi-monochromatic LEDs (474 and 600 nm), which, when being combined with a basic white LED (Cree CMA 2550), allow controlling the widest CCT range. Quasi-monochromatic LEDs with particular optimal spectral parameters allow adjusting CCT within the range from 3098 up to 6712 K, while maintaining a high color rendering index (higher than 80) over the most part (3098 to 5600 K) of the regulation range.

Keywords: LED, tunable white light, artificial lighting, correlated color temperature, Duv, color rendering index.

<https://doi.org/10.15407/spqeo25.03.303>

PACS 42.72.-g, 52.80.Mg, 85.60.Jb, 92.60.Pw

Manuscript received 02.04.22; revised version received 16.08.22; accepted for publication 21.09.22; published online 06.10.22.

1. Introduction

Designing a comfortable lighting environment for humans is an integral part of creating good work and leisure conditions [1, 2]. Spectral characteristics and intensity of illumination in the closest environment affect the secretion of such hormones as melatonin and cortisol, which significantly impact the health and psychophysiological state of a person. In the natural environment (with no artificial light sources), the level of melatonin in the human body begins gradually increasing just after nightfall, and then gradually decreases, reaching its day time level by dawn [3, 4].

When changes in the natural cycles of spectral composition of light are significantly disrupted by the artificial lighting, human biorhythms become desynchronized, which causes sleep disorders, excessive emotional stress, reduces productivity and, eventually, leads to chronic diseases [5, 6]. Light of a certain spectral composition is used to address the lack of vitamin D [7], which can in fact be considered as a mean to prevent viral diseases (COVID-19 in particular [8]). It is worth

noting that a person's well-being gains greatly from periodical exposure to bright daylight or an artificial lighting as close to the natural one as possible.

That is why creating high-power lighting systems capable of synthesizing light similar to daylight with parameters that can be adjusted throughout the day is a very important task for the subject-matter experts. Such lighting systems can provide the desired spectral characteristics, if using them to illuminate rooms with no natural insolation.

LED lighting systems made up of LEDs with different spectral characteristics can provide lighting with a widely tunable spectral range of the synthesized light [9], which makes them suitable for both general lighting and special decorative or accent lighting of individual interior elements.

Quality of light can be defined by a number of standard parameters, the specifications for which are generally accepted among the experts or prescribed by regulations. A number of indicators are used to determine reliability of color rendering inherent to light sources.

These indicators enable to quantify quality of synthesized light. The most common parameter that characterizes the similarity of synthesized light to natural light is the color rendering index (CRI or R_a) [10].

To increase reliability of the light quality assessment, Illuminating Engineering Society (IES) developed new indicators, namely: the fidelity index (IES R_f), the gamut index (IES R_g) [11, 12], and the Color Quality Scale (CQS) [13] have been proposed by the National Institute of Standards and Technology. The International Commission on Illumination (Commission internationale de l'éclairage, CIE) recommends using IES R_f and IES R_g [14] and, in some cases, CQS as well instead of R_a , because they can provide a more accurate estimate of color rendering quality. At the same time, numerous studies [15–17] indicate that even if high values of these parameters are achieved, the impact on the human body is mainly defined by the correlated color temperature (CCT), which is a significant parameter of the light effect on the human body.

Creating high lighting levels requires using high-power lighting systems. Lately, high-power LED lighting fixtures have been built with high-power LEDs and COB (chip-on-board) LEDs [18]. When there is a need to create a lighting fixture with a power higher than the power of individual LEDs or able to be adjusted, the spectral composition of the resulting light, LEDs and COB LED modules are assembled into LED clusters [19]. LED clusters may include LEDs with different spectral characteristics and have a capability to control the luminous intensity of individual LEDs or their groups.

Modern technological solutions used to create new high-power LEDs and COB LED modules allow building high and ultra-high power lighting fixtures that use one [20] or several [21] high-power LED light sources. At the same time, the scope of the applied LED lighting devices requires that their design combines high reliability and manufacturability, low power and material consumption, modern exterior and the ability to be powered from renewable energy sources [22].

Rapid increase in the power of individual LEDs and COB LED modules designed to ensure high light quality requires to use new efficient cooling systems based on two-phase heat-transfer devices with an effective thermal conductivity far exceeding the thermal conductivity of homogeneous materials [27–29]. Moreover, the use of new materials (such as macroporous silicon [30, 31]) and manufacturing technologies (*e.g.*, organic LEDs [32, 33]) further increases the power and decreases the cost of LEDs, which significantly expands the application scope of high-power LED lighting fixtures.

An important aspect of expanding the application scope of high-power LED clusters is to ensure the tunability of the spectral composition of resulting light with high quality parameters. There are different types of LED clusters with tunable CCT, including those based on two, three, four or five types of LEDs [34]. The most common LED clusters consist of red, green and blue (RGB) diodes. LED clusters based on four types of LEDs

are usually called RGBx, where x stands for A (amber), Y (yellow) or W (white). By using several types of LEDs with different spectral power distribution (SPD), it is possible to obtain a lighting system capable of smoothly changing SPD for the resulting light and its characteristics (CCT, Duv, R_a *etc.*). Increasing the number of LEDs of a certain spectral composition in a cluster allows one to expand the capabilities of the latter in synthesizing the light of a given spectral composition as well as to improve quality of synthesized light.

Synthesizing the light with particular spectral parameters requires matching the power of different types of LEDs and creating control algorithms, which would be a most effective with the known types of LEDs. The known literature data describe LED clusters based on LEDs of two [35] or three [36] types, which use nonlinear empirical models for determining the power of individual types of LEDs [37, 38]. These systems are built using commercial LEDs, and their capabilities for light synthesis are limited by the spectral characteristics of the chosen types of LEDs. At the same time, modern industry can produce quasi-monochromatic and broadband visible-range LEDs with accurately determined spectral parameters (peak wavelengths (PW) and SPD). If being optimally selected, these diodes will provide high light efficiency and a wide CCT range of the lighting system.

This study is aimed at determining the optimal parameters of quasi-monochromatic LEDs for high-power LED clusters with tunable CCT and demonstrating the possibility of their use in LED clusters providing near-natural synthesized light conditions.

2. Choosing a base high-power white LED light source

One of the ways to design high-power LED lighting systems is to use white ultra-high power COB LED modules, which are widely produced by global manufacturers of LED light sources. Their power may exceed 500 W [39], and the efficiency can reach 140...180 lm/W [40], which reduces the total number of LEDs in the lighting system. Today, however, most of these high-power LED modules have a low CRI, which limits their application in rooms that require to use high- R_a lighting fixtures. The color rendering index is increased by continuously adding the RGB component to the resulting light, which usually reduces the light efficiency of the lighting system as a whole.

Another way to design these devices is to use commercially available LEDs with R_a over 90. Such COB modules usually have a nominal power of 50...104 W, so to create an ultra-high power lighting systems (200 W or more), several such COB LED modules must be assembled in a cluster. An important advantage of COB LED modules with a maximum power close to 100 W is their low supply voltages (less than 40 V), which increases their reliability and simplifies their systems for power supply from renewable energy sources, namely, solar panels [20, 21].

When creating powerful lighting systems, it is the best way to reduce the contribution of quasi-monochromatic LEDs due to their lower light efficiency and luminous flux. It is also advisable to reduce the total number of LEDs and their control channels in the cluster. To reduce the light flux component of quasi-monochromatic LEDs in the resulting light, the base white LED must have such parameters that would in the most of cases allow it to operate as a standalone diode or with a small quasi-monochromatic component, and, when CCT needs to be changed, to function effectively together with low-power quasi-monochromatic diodes.

Given that this work was aimed at developing the lighting systems with a tunable CCT capable of providing high color rendering at high light efficiency, a preliminary study was carried out on the light and spectral parameters of commercially available and common white LEDs and COB LED modules, as well as a number of quasi-monochromatic LED modules. Spectral parameters were determined using the modern metrological equipment available at the V. Lashkaryov Institute of Semiconductor Physics, NAS of Ukraine, *i.e.*, a CAS-140 matrix spectroradiometer (Instrument system, Germany) and an integrating sphere 2 m in diameter. The HAMEG HMP4040 power supply unit manufactured by Rohde & Schwarz (Germany) was used for power supply and for determining electrical parameters of LEDs (current, voltage, power).

According to the research results, CMA2550 COB LED modules by Cree were found to be among the most effective white LED light sources [41] capable of providing both high light efficiency and high light quality. The normalized spectrum of such COB LED modules (Fig. 1) is typical of white LEDs, except for quasi-monochromatic peaks at the wavelengths 608.5, 613.5, 631.0, 635.3 and 647.5 nm, which are used to achieve high light efficiency at high R_a [42–44].

CCT of the chosen LED, which is about 4000 K, is the most common for rooms with a constant presence of people. It means that in most of cases, this system can operate using only the radiation of white COB LED module. Adding extra radiation of quasi-monochromatic LEDs of a certain spectral composition to the base white COB module allows changing CCT of the resulting light.

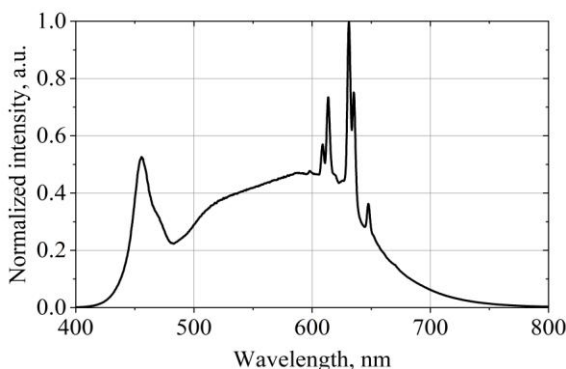


Fig. 1. Normalized SPD of the Cree CMA2550 basic white COB LED module used in the study.

3. Calculation technique for spectral parameters of synthesized light

Synthesizing light with CCT lower than the base white light requires adding a long-wavelength quasi-monochromatic component (575...650 nm) to the resulting light, while increasing CCT requires adding a short-wavelength component (450...500 nm). When using only two LEDs (white and quasi-monochromatic) at the same time, their color coordinates shift on the CIE chromaticity diagram in a straight line (Fig. 2), which connects these color coordinates (lines BW and WR). It is this shift in the color coordinates that changes CCT of the synthesized light.

If the distance between the chromaticity coordinates of the resulting light and the Planckian curve (parameter $\Delta u, v$, or Duv) exceeds 0.006 units, the calculation of the color parameters of the synthesized light is considered incorrect. Thus, when performing calculations, the parameter Duv should be taken into consideration. To approximate the chromaticity coordinates of the synthesized light to the Planckian curve coordinates, tetrachromatic systems use a green LED. Using the green LED in a cluster allows for a slight expansion of the color coordinates range, but also complicates the structure of such a cluster.

SPD is synthesized ($P_\lambda(\lambda)$) from particular LEDs spectra by summing their intensity over all the wavelengths:

$$P_\lambda(\lambda) = k_1 P_{1\lambda}(\lambda) + k_2 P_{2\lambda}(\lambda), \quad (1)$$

where k_1 and k_2 are coefficients determining the parts of radiation in the resulting light of the LED spectra with the spectral distributions $P_{1\lambda}(\lambda)$ and $P_{2\lambda}(\lambda)$, respectively.

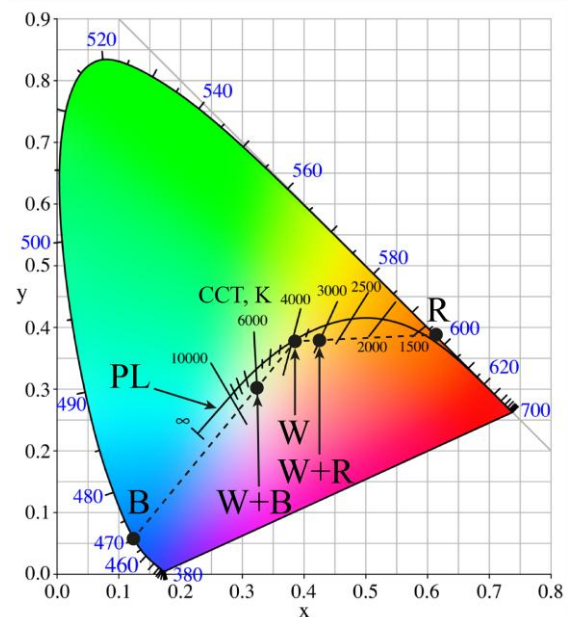


Fig. 2. CIE xy chromaticity diagram with the chromaticity coordinates of R, B and W LEDs and an example of obtaining color coordinates of light on the Planckian locus (PL), when the light is synthesized using RW and BW components.

It was assumed that:

$$k_1 + k_2 = 1. \quad (2)$$

The spectral parameters (CCT, Duv, R_a , IES R_f , IES R_g , CQS) of the resulting light, on the other hand, are defined using complex mathematical calculations and cannot be described by simple mathematical dependences.

The technique for determining the color temperature was developed by the CIE in 1931 [45]. Determined were the matching functions of chromaticity coordinates (x , y , z), which characterize the light color perception by the average person, and the methods that allow finding CCT based on the spectral distribution of light. The color matching functions were chosen so that the intensities of red (\bar{x}), green (\bar{y}) and blue (\bar{z}) corresponded to monochromatic light over the entire visible spectrum of radiation, while the green matching function was assumed to be equal to the human eye sensitivity function.

For a certain spectral distribution of radiation, the light chromaticity coordinates are calculated in the CIE color space (1931):

$$X = k_c \int_0^{\infty} P_{\lambda}(\lambda) \bar{x}(\lambda) d\lambda, \quad (3)$$

$$Y = k_c \int_0^{\infty} P_{\lambda}(\lambda) \bar{y}(\lambda) d\lambda, \quad (4)$$

$$Z = k_c \int_0^{\infty} P_{\lambda}(\lambda) \bar{z}(\lambda) d\lambda, \quad (5)$$

where k_c is the coefficient calculated as:

$$k_c = \frac{100}{\int_0^{\infty} P_{\lambda}(\lambda) \bar{y}(\lambda) d\lambda}. \quad (6)$$

When the purpose of calculations is to determine the chromaticity coordinates, the total factor k_c can be ignored, because it will be cancelled in the process of calculations. CCT is normally found using chromaticity coordinates in the CIE 1960 color space (u , v) [46]. The chromaticity coordinates u and v can be calculated using the following equations:

$$u = \frac{4X}{X + 15Y + 3Z}, \quad (7)$$

$$v = \frac{6X}{X + 15Y + 3Z}, \quad (8)$$

The additional chromaticity coordinate L that characterizes the brightness of light source is equated to the chromaticity coordinate Y .

Subsequently, the chromaticity coordinates of light can be used to calculate CCT by using the methods based on tables (Robertson's method [47]) or the approximated third-order polynomial (McCamy's method [48]).

In 2013, Yoshi Ohno [49] proposed three techniques to calculate CCT: the triangular solution, the parabolic solution and the combined solution. All of them are based on using the table with values of blackbody temperatures in increments of 1% from 1000 to 20168 K with the corresponding temperatures and chromaticity coordinates (u , v). The proposed methods allow determining CCT within the range from 2000 up to 20000 K at $-0.03 < \text{Duv} < 0.03$ with a maximum error of 0.8 K.

For $\text{Duv} < 0.02$, the said method proposes to use the triangle technique as an approximation. This technique involves the calculation of distance between the light and blackbody chromaticity coordinates found from the calculation table. Next, the determined value of minimum distance is used to find the nearest CCT $-T_m$, as well as the two neighboring values (T_{m-1} , T_{m+1}). Using linear interpolation and applying the correction factor of 0.99991 for 1% temperature increment, CCT of the studied light source is determined for T_{m-1} and T_{m+1} rows of the table by using the following equations:

$$l = \sqrt{(u_{m+1} - u_{m-1})^2 + (v_{m+1} - v_{m-1})^2}, \quad (9)$$

$$x = \frac{d_{m+1}^2 - d_{m-1}^2 + l^2}{2l}, \quad (10)$$

$$T_x = T_{m-1} + \frac{(T_{m+1} - T_{m-1})x}{l}, \quad (11)$$

$$\text{CCT} = T_x \cdot 0.999. \quad (12)$$

The calculation of Duv in accord with the classical CIE method involves comparing the chromaticity coordinates of the blackbody having CCT of the studied light source with the chromaticity coordinates of the latter. Yoshi Ohno proposed to calculate by Duv simpler dependences [49], which allow using only the chromaticity coordinates, and thus speed up the calculation:

$$L_{FP} = (u - 0.292)^2 + (v - 0.240)^2, \quad (13)$$

$$a = \arccos(u - 0.292L_{FP}), \quad (14)$$

$$L_{BB} = k_6 a^2 + k_5 a^5 + k_4 a^4 + k_3 a^3 + k_2 a^2 + k_1 a + k_0, \quad (15)$$

$$\text{Duv} = L_{FP} - L_{BB}, \quad (16)$$

where $k_6 = -0.00616793$, $k_5 = 0.0893944$, $k_4 = -0.5179722$, $k_3 = 1.5317403$, $k_2 = -2.4243787$, $k_1 = 1.925865$, and $k_0 = -0.471106$.

The R_a , IES R_f , IES R_g and CQS parameters are determined using a principle of calculating the color distortion of the selected reference color samples illuminated with the studied light source relative to them being illuminated by the Planckian emitter with the same CCT.

It is this difference between the chromaticity coordinates for the i^{th} color reference sample illuminated with the studied light source and Planckian emitter that determines the color difference of the reference surface illuminated with the studied light source relative to the illuminated Planckian emitter. The color difference (ΔE_i^*) for the i^{th} color reference sample is determined as follows [10]:

$$\Delta E_i^* = \sqrt{(\Delta L_i^{**})^2 + (\Delta u_i^{**})^2 + (\Delta v_i^{**})^2}, \quad (17)$$

where ΔL_i^{**} , Δu_i^{**} , Δv_i^{**} are the corresponding differences in chromaticity coordinates after color shift. R_a is calculated using 8 primary reference colors and six additional saturated reference colors (used to further characterize light sources). For the i^{th} reference color, the corresponding CRI_i value is found in the following manner:

$$R_i = 100 - 4.6 \cdot \Delta E_i^*. \quad (18)$$

Accordingly, the full color rendering index is calculated using the equation:

$$R_a = \frac{1}{N} \cdot \sum_{i=1}^N CRI_i. \quad (19)$$

CQS is calculated similarly to R_a , but it uses fifteen saturated colors, which are more prone to distortion under artificial lighting. The method of calculating color distortion has been changed and optimized so that high distortion by one of the templates did not make the total index value to remain high.

This method of determining CQS [13] has some drawbacks. It is known that the characteristic properties of the spectrum of emitted light have a certain effect on the color perception, making the colors visually brighter or dimmer. Thus, both saturation and tone of a hue are important characteristics, but the CQS method does not take them into consideration. This shortcoming can be amended by introducing a new parameter and increasing the number of reference samples.

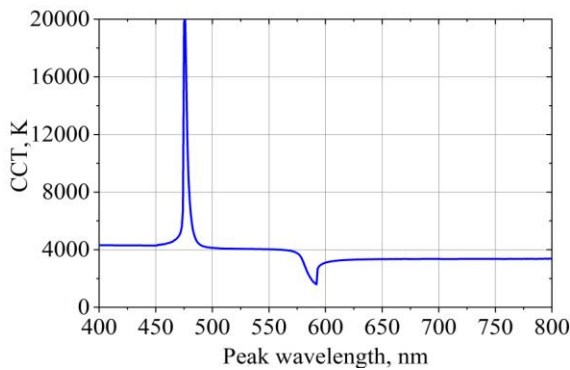


Fig. 3. Dependence of the maximum and minimum CCT at the peak wavelength of quasi-monochromatic LED used in this study.

The IES R_f calculation [11] now uses 99 reference samples, which significantly increases the reliability of determining the color rendering quality over the entire color range, and the additional parameter IES R_g allows determining the color saturation.

The resulting spectra and their parameters were determined with a software developed for this specific purpose. The software allowed performing the necessary analytical operations by using the experimentally determined spectra of white LEDs and software-generated spectra of quasi-monochromatic LEDs. The latter with the peak wavelengths from 400 up to 800 nm in 1 nm increments were software-generated as based on experimentally measured spectra of quasi-monochromatic LEDs manufactured by Cree with the peak wavelengths 455, 522 and 629 nm (spectral halfwidth 17...40 nm).

The LuxPy software package both implements the use of Yoshi Ohno method for determining CCT and Duv and applies the generally accepted standards and methods to determine the R_a , IES R_f , IES R_g and CQS parameters [10–13].

The software uses the Python LuxPy package [50], which provides comprehensive information on the spectral parameters of the synthesized light. Moreover, hundreds of random calculation results were used to verify the obtained data by using the well-known LED ColorCalculator software [51].

4. Optimizing SPD of quasi-monochromatic LEDs

The developed software was used to simulate and determine the peak wavelengths of quasi-monochromatic LEDs, which enabled to synthesize spectra in the widest possible CCT range (Fig. 3) simultaneously keeping the Duv value below 0.006.

For the ranges in the neighborhood of the extremums of CCT vs peak wavelength dependence of the quasi-monochromatic LED, the dependences were found for the qualitative parameters of the synthesized light on the quasi-monochromatic LEDs. Fig. 4 shows the dependences of R_a , IES R_f , IES R_g , CQS for CCT of the resulting light: 3100, 3300, 3500, 3700, 4500, 5000, 5500 and 6000 K. Table 1 shows the spectral parameters of the synthesized light at the end points of the presented curves, as well as without any additional quasi-monochromatic component.

For lighting systems designed to synthesize light similar to daylight, it is important to be able to change CCT from 3000...3100 up to 5500...6000 K, which is a typical range for natural daylight. Fig. 5 shows the dependences of CCT of the resulting light for the selected base white LED and quasi-monochromatic blue and red spectrum LEDs. The nature of these dependences demonstrates that a quasi-monochromatic LED with a shorter peak wavelength (474 nm) can increase CCT of the resulting light. To reduce CCT, on the other hand, it is more efficient to use a quasi-monochromatic LED with a longer peak wavelength (600 nm).

The steeper the dependence of CCT for the resulting light on the contribution of quasi-monochromatic LED

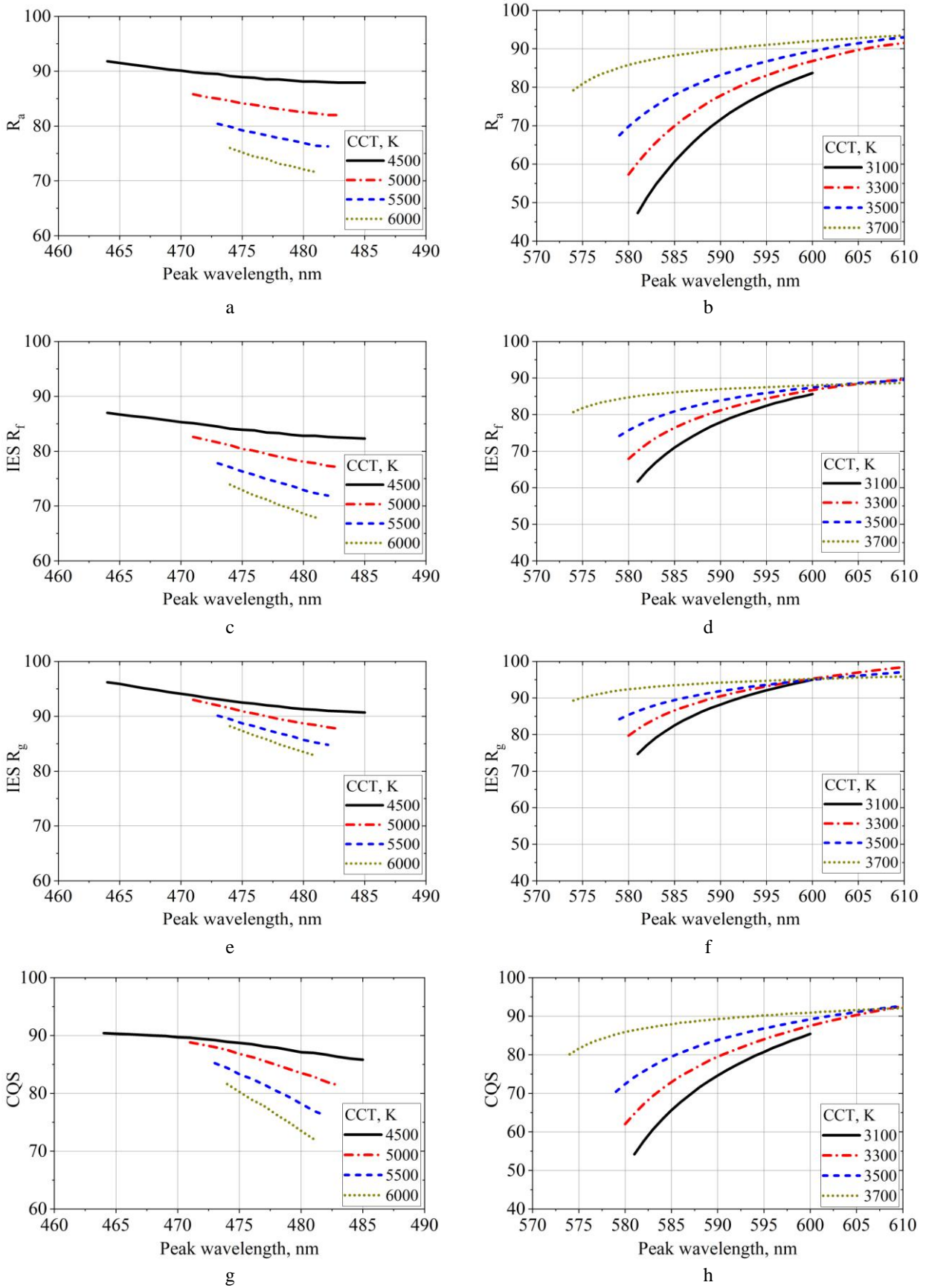


Fig. 4. Dependences of R_a (a, b), $IES R_f$ (c, d), $IES R_g$ (e, f), CQS (g, h) on the peak wavelength of the quasi-monochromatic LED used in studying the maximum achievable CCT values.

Table 1. Spectral parameters of the synthesized light when using the quasi-monochromatic LEDs with the peak wavelengths 474 and 600 nm.

CCT, K	PW, nm	R_a	IES R_f	IES R_g	CQS
3100	581	47.3	61.7	74.7	54.2
	600	83.7	85.6	95.0	85.4
3300	580	57.3	67.9	79.7	62
	823	93.4	91.3	101.3	96.1
3500	579	67.5	74.2	84.2	70.4
	800	81.5	78.1	100.5	81.9
3700	574	79.2	80.7	89.3	80.1
	800	93.1	87.7	97	90.4
3953	–	92.6	88.1	95.1	91.4
4500	464	91.8	87.0	96.2	90.4
	485	87.9	82.3	90.7	85.8
5000	471	85.8	82.6	93.0	88.8
	483	82.0	77.1	87.7	81.4
5500	473	80.4	77.8	90.1	85.2
	482	76.3	71.9	84.8	76.1
6000	474	76.0	73.9	88.2	81.6
	481	71.6	67.9	82.8	72.1

Table 2. Spectral parameters of synthesized light at the end points of R_a , IES R_f , IES R_g and CQS curves.

CCT, K	Quasi-monochromatic component, %	Duv	R_a	IES R_f	IES R_g	CQS
3098	15.5	0.0059	83.7	85.6	95.0	85.4
3200	13.4	0.0050	85.3	86.2	95.1	86.5
3500	7.6	0.0019	89.5	87.4	95.0	89.2
4500	2.6	0.0012	89.3	84.3	92.8	89.0
5000	4.5	0.0034	84.6	81.1	91.5	87.5
5500	6.1	0.0047	80.2	77.4	89.6	84.6
6000	7.4	0.0055	76.0	73.9	88.2	81.6
6712	9.0	0.0059	71.4	70.1	86.1	78.1

(Fig. 5), the smaller the contribution of the quasi-monochromatic LED is required to obtain certain CCT. The nature of the dependence of CCT on the contribution of different types of quasi-monochromatic LEDs indicates that shorter-wavelength LEDs will minimize the contribution and thus increase CCT more effectively, while longer-wave LEDs will reduce CCT.

The analysis of dependences shown in Fig. 5 allows us to conclude that LEDs with 474 and 600 nm peak wavelengths enable to tune CCT within the range 3100...6000 K. The range from 3100 up to 5500 K allows for R_a higher than 80. Further increasing CCT up to 6700 K reduces R_a down to 72, which is also an allowable value. In the vast majority of cases, these systems operate within the range 3500...4500 K, where application of selected quasi-monochromatic LEDs retains R_a over 90.

5. Simulating radiation spectra of LED clusters

The values of the spectral parameters of the synthesized light (Fig. 6) and the contribution of quasi-monochromatic LEDs in the resulting light (Fig. 7) for different CCT were calculated for the selected types of LEDs. Table 2 presents the simulation results for these parameters for different CCTs: 3200, 3500, 4000, 4500, 5000, 5500, 6000 K, as well as for the end points of the curves presented above (3098 and 6712 K). Figs 6 and 7 and Table 2 present the data for the Duv parameter of synthesized light below 0.006. It should be noted that a further increase in the contribution of quasi-monochromatic LEDs leads to a further decrease or increase in CCT, but in this case Duv exceeds 0.006, which does not allow for accurate determination of the color parameters.

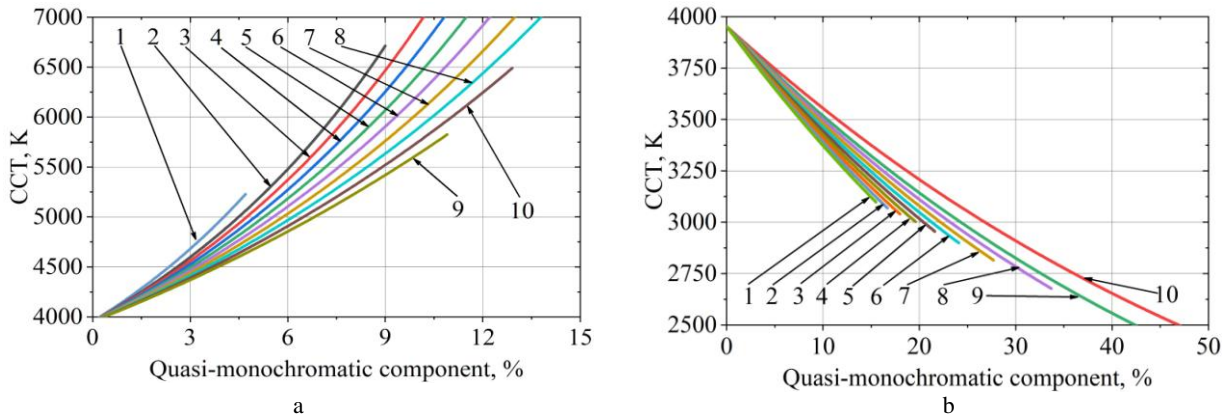


Fig. 5. Dependences of CCT of the resulting light on the contribution of quasi-monochromatic LED radiation of short-wavelength (a, where 472 (1), 474 (2), 475 (3), 476 (4), 477 (5), 478 (6), 479 (7), 480 (8), 481 (9), and 482 (10) nm) and long-wavelength (b, where 590 (1), 592 (2), 593 (3), 594 (4), 595 (5), 596 (6), 597 (7), 598 (8), 599 (9), and 600 (10) nm) spectral ranges in the resulting radiation.

Our analysis of the dependences shown in Fig. 6 indicates that when the peak wavelength of additional quasi-monochromatic LEDs changes, the R_a value is the most decreased, down to 22.8%, while IES R_f is decreased by 20.5%, R_g by 9.5%, and CQS by 14.6%. Fig. 7 and Table 2 demonstrate that most of the luminous flux (15.5%) of the quasi-monochromatic LEDs is used to synthesize the light with CCT close to 3098 K.

When the light efficiency of the quasi-monochromatic LEDs is 2...2.5 times lower than that of the base white LED, which is typical for these LEDs with the peak wavelengths within this spectral range (around 600 nm), the light efficiency of this cluster is reduced by no more than 13.5...18.1%. When CCT of 6712 K is reached, the luminous flux of the quasi-monochromatic LED is 9%, but quasi-monochromatic LEDs with the peak wavelength close to 474 nm tend to have a light efficiency that is 3...3.5 times lower than that of the base white LED, which corresponds to a decrease in the light efficiency 15.1...18.3% of the whole LED.

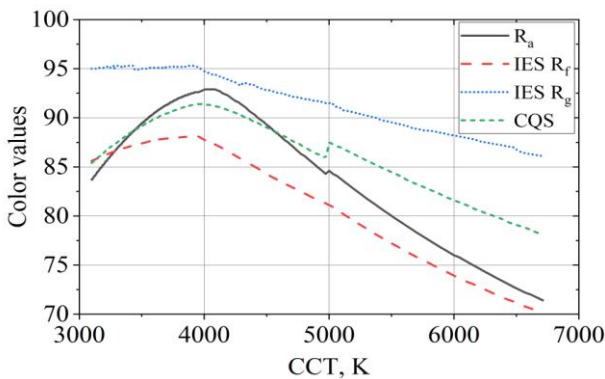


Fig. 6. Dependences of color parameters inherent to the LED cluster on CCT when using quasi-monochromatic LEDs with the peak wavelengths 474 and 600 nm.

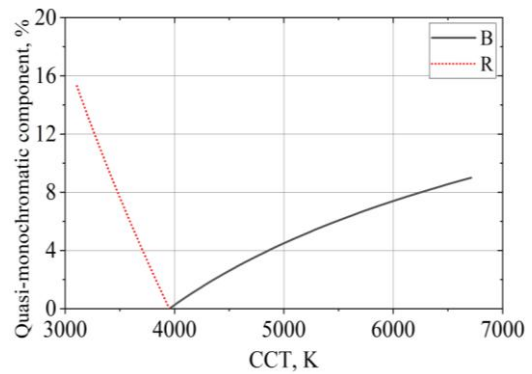


Fig. 7. Dependence of the luminous flux component inherent to quasi-monochromatic LEDs with the peak wavelengths 474 nm (B) and 600 nm (R) in the resulting luminous flux on CCT.

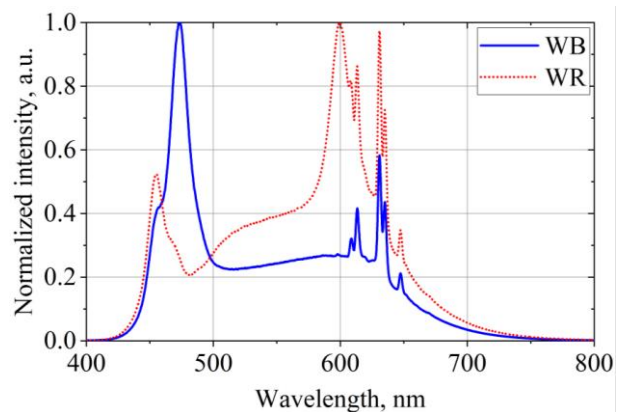


Fig. 8. Normalized SPDs of resultant light for maximum achievable CCTs of 3098 K (WB) and 6712 K (WR) when combining radiation from a selected base white LED with selected quasi-monochromatic LEDs (peak wavelengths 474 and 600 nm).

The normalized spectral distributions of synthesized light for the maximum achievable CCTs (3098 and 6712 K) shown in Fig. 8 indicate a significant decrease in the intensity of radiation in the green spectral range (520...565 nm) in the synthesized light as compared with the basic white LED (Fig. 1), which is the reason for the decrease in quality of the synthesized light.

The obtained research results allow assuming that the use of traditional combinations or specialized broadband LEDs instead of quasi-monochromatic LEDs will increase quality of resulting white light over the entire CCT range.

6. Conclusions

1. The study has determined optimal peak wavelengths of quasi-monochromatic LEDs (474 and 600 nm) for LED clusters with tunable correlated color temperature, which allow for the widest possible adjustment range.

2. Using a CMA 2550 basic white COB LED module manufactured by Cree as an example, the study has shown that adding quasi-monochromatic LEDs radiation with the peak wavelengths 474 and 600 nm to the resulting light allows adjusting the correlated color temperature within the range 3100 to 5500 K, while maintaining R_a within the range 95 to 80. A further increase in the CCT range to 6700 K reduces R_a to 72, which is also acceptable in some cases.

3. The light efficiency of the lighting system based on the developed LED cluster is reduced relative to the base white LED by no more than 18.3% within the range of correlated color temperatures 3098...6712 K.

4. Further studies should address the search for spectra of quasi-monochromatic LED combinations that can provide a high R_a with a wide CCT range.

References

1. Ticleanu C. Impacts of home lighting on human health. *Lighting Res. Technol.* 2021. **53**, No 5. P. 453–475. <https://doi.org/10.1177/14771535211021064>.
2. Nagare R., Woo M., MacNaughton P. *et al.* Access to daylight at home improves circadian alignment, sleep, and mental health in healthy adults: A crossover study. *Int. J. Environ. Res. Public Health.* 2021. **18**, No 19. Art. No 9980. <http://dx.doi.org/10.3390/ijerph18199980>.
3. von Gall C. The effects of light and the circadian system on rhythmic brain function. *Int. J. Molecul. Sci.* 2022. **23**, No 5. Art. No 2778. <https://doi.org/10.3390/ijms23052778>.
4. Pandi-Perumal S.R., Cardinali D.P., Zaki N.F.W. *et al.* Timing is everything: Circadian rhythms and their role in the control of sleep. *Frontiers in Neuroendocrinology.* 2022. **66**. Art. No 100978. <https://doi.org/10.1016/j.yfrne.2022.100978>.
5. Al-Naggar R.A., Anil S. Artificial light at night and cancer: Global study. *Asian Pacific Journal of Cancer Prevention.* 2016. **17**, No 10. P. 4661–4664. <https://doi.org/10.7314/APJCP.2016.17.10.4661>.
6. Svechkina A., Portnov B.A., Trop T. The impact of artificial light at night on human and ecosystem health: a systematic literature review. *Landscape Ecol.* 2020. **35**, P. 1725–1742. <https://doi.org/10.1007/s10980-020-01053-1>.
7. Wacker M., Holick M.F. Sunlight and vitamin D. *Dermato-Endocrinology.* 2013. **5**, No 1. P. 51–108. <http://dx.doi.org/10.4161/derm.24494>.
8. Nakano T., Chiang K.C., Chen C.C. *et al.* Sunlight exposure and phototherapy: Perspectives for healthy aging in an era of COVID-19. *Int. J. Environ. Res. Public Health.* 2021. **18**, No 20. Art. No 10950. <https://doi.org/10.3390/ijerph182010950>.
9. Nie J., Wang Q., Dang W. *et al.* Tunable LED lighting with five channels of RGCWW for high circadian and visual performances. *IEEE Photonics J.* 2019. **11**, No 6. Art. No 8201512. <https://doi.org/10.1109/JPHOT.2019.2950834>.
10. CIE13.3-1995. 1995. Method of measuring and specifying colour rendering properties of light sources. Vienna (Austria): CIE.
11. David A., Fini P.T., Houser K.W. *et al.* Development of the IES method for evaluating the color rendition of light sources. *Opt. Exp.* 2015. **23**. P. 15888–15906. <https://doi.org/10.1364/OE.23.015888>.
12. IES. 2015. IES-TM-30-15: method for evaluating light source color rendition. New York (NY): The Illuminating Engineering Society of North America.
13. Davis W., Ohno Y. Color quality scale. *Opt. Eng.* 2010. **49**. P. 33602–33616.
14. CIE13.3-1995. 1995. Method of measuring and specifying colour rendering properties of light sources. Vienna (Austria): CIE.
15. Zhu Y., Yang M., Yao Y. *et al.* Effects of illuminance and correlated color temperature on daytime cognitive performance, subjective mood, and alertness in healthy adults. *Environment and Behavior.* 2017. **51**, No 2. P. 199–230. <http://dx.doi.org/10.1177/0013916517738077>.
16. Lan L., Hadji S., Xia L. *et al.* The effects of light illuminance and correlated color temperature on mood and creativity. *Build. Simul.* 2021. **14**. P. 463–475. <https://doi.org/10.1007/s12273-020-0652-z>.
17. LiY., Ru T., Chen Q. *et al.* Effects of illuminance and correlated color temperature of indoor light on emotion perception. *Sci. Rep.* 2021. **11**. Art. No 14351. <https://doi.org/10.1038/s41598-021-93523-y>.
18. Lishik S.I., Posedko V.S., Trofimov Yu.V., Tsvirko V.I. Current state, trends and perspectives of the development of light emitting diode technology. *Light & Eng.* 2017. **25**. P. 13–24.
19. Zhang M., Chen Y., He G. Color temperature tunable white-light LED cluster with extrahigh color rendering index. *The Scientific World Journal.* 2014. **2014**. Art. No 897960. <https://doi.org/10.1155/2014/897960>.
20. Pekur D.V., Sorokin V.M., Nikolaenko Yu.E. *et al.* Electro-optical characteristics of an innovative LED luminaire with an LED matrix cooling system based on heat pipes. *SPQEO.* 2020. **23**, No 4. P. 415–423. <https://doi.org/10.15407/spqeo23.04.415>.

21. Pekur D.V., Kolomzarov Yu.V., Sorokin V.M., Nikolaenko Yu.E. Super powerful LED luminaires with a high color rendering index for lighting systems with combined electric power supply. *SPQEO*. 2022. **25**, No 1. P. 97–107. <https://doi.org/10.15407/spqeo25.01.097>.
22. Kornaga V.I., Pekur D.V., Kolomzarov Yu.V. *et al.* Intelligence system for monitoring and governing the energy efficiency of solar panels to power LED luminaires. *SPQEO*. 2021. **24**, No 5. P. 200–209. <https://doi.org/10.15407/spqeo24.02.200>.
23. Nikolaenko Yu.E., Pekur D.V., Sorokin V.M. Light characteristics of high-power LED luminaire with a cooling system based on heat pipe. *SPQEO*. 2019. **22**, No 3. P. 366–371. <https://doi.org/10.15407/spqeo22.03.366>.
24. Pekur D.V., Nikolaenko Yu.E., Sorokin V.M. Optimization of the cooling system design for a compact high-power LED luminaire. *SPQEO*. 2020. **23**, No 1. P. 91–101. <https://doi.org/10.15407/spqeo23.01.091>.
25. Pekur D.V., Sorokin V.M., Nikolaenko Yu.E. Thermal characteristics of a compact LED luminaire with a cooling system based on heat pipes. *TSEP*. 2020. **18**. Art. No 100549. <https://doi.org/10.1016/j.tsep.2020.100549>.
26. Pekur D.V., Sorokin V.M., Nikolaenko Y.E. Features of wall-mounted luminaires with different types of light sources. *ELECTRICA*. 2021. **21**, No 1. P. 32–40. <https://doi.org/10.5152/electrica.2020.20017>.
27. Reay D.A., Kew P.A., McGlen R.J. *Heat Pipe: Theory, Design and Applications*. 6th ed. Butterworth-Heinemann, Amsterdam, 2014. <https://doi.org/10.1016/C2011-0-08979-2>.
28. Prisiakov K., Marchenko O., Melikaev Yu. *et al.* About complex influence of vibrations and gravitational fields on serviceability of heat pipes in composition of the space-rocket systems. *54th Int. Astronautical Congress of the Int. Astronautical Federation (IAF), the Int. Academy of Astronautics and the Int. Institute of Space Law, Int. Astronautical Congress (IAF)*. Bremen, Germany, 2003. P. 1571–1580. <https://doi.org/10.2514/6.IAC-03-I.1.10>.
29. Nikolaenko Yu.E., Pekur D.V., Sorokin V.M. *et al.* Experimental study on characteristics of gravity heat pipe with threaded evaporator. *TSEP*. 2021. **26**. Art. No 101107. <https://doi.org/10.1016/j.tsep.2021.101107>.
30. Gentsar P.O., Stronski A.V., Karachevtseva L.A., Onyshchenko V.F. Optical properties of monocrystalline silicon nanowires. *Physics and Chemistry of Solid State*. 2021. **22**, No 3. P. 453–459. <https://doi.org/10.15330/pssc.22.3.453-459>.
31. Onyshchenko V.F. Distribution of excess charge carriers in bilateral macroporous silicon with different thicknesses of porous layers. *J. Nano-Electron. Phys.* 2021. **13**, No 6. P. 06010-1–06010-5. [https://doi.org/10.21272/jnep.13\(6\).06010](https://doi.org/10.21272/jnep.13(6).06010).
32. Posudievsky O.Y., Lypenko D.A., Khazieieva O.A. *et al.* Nanocomposite of polyaniline with partially oxidized graphene as the transport layer of light-emitting polymer diodes. *Theoretical and Experimental Chemistry*. **50**, No 2. P. 96–102. <https://doi.org/10.1007/s11237-014-9352-z>.
33. Cherpak V., Stakhira P., Khomyak S. *et al.* Properties of 2,6-di-tert.-butyl-4-(2,5-diphenyl-3,4-dihydro-2H-pyrazol-3-yl)-phenol as hole-transport material for life extension of organic light emitting diodes. *Opt. Mater.* 2011. **33**, No 11. P. 1727–1731. <https://doi.org/10.1016/j.optmat.2011.05.034>.
34. Zhan X., Wang W., Chung H. A novel color control method for multi-color LED systems to achieve high color rendering indexes. *IEEE Trans. Power Electron.* 2018. **33**, No 10. P. 8246–8258. <https://doi.org/10.1109/TPEL.2017.2785307>.
35. Qiao L., Zhang H., Yu J. *et al.* Design of smart light source based on bi-color LED with single duty cycle for correlated color temperature adjustment. *Opt. Quant. Electron.* 2021. **53**, No 11. P. 610. <http://dx.doi.org/10.1007/s11082-021-03227-w>.
36. Wong C.P.G., Lee A.T.L., Li K. *et al.* Precise luminous flux and color control of dimmable red-green-blue light-emitting diode systems. *IEEE Trans. Power Electron.* 2022. **37**, No 1. P. 588–606. <http://dx.doi.org/10.1109/tpel.2021.3102260>.
37. Lee A.T.L., Chen H., Tan S.-C. Hui S.Y. Precise dimming and color control of LED systems based on color mixing. *IEEE Trans. Power Electron.* 2016. **31**, No 1. P. 65–80. <https://doi.org/10.1109/tpel.2015.2448641>.
38. Chen H., Tan S., Lee A., Lin D., Hui S. Precise color control of red-green-blue light-emitting diode systems. *IEEE Trans. Power Electron.* 2017. **32**, No 4. P. 3063–3074. <https://doi.org/10.1109/TPEL.2016.2581828>.
39. CITIZEN ELECTRONICS CO., LTD. https://ce.citizen.co.jp/cms/ce/lighting_led/dl_data/COB_Version6/datasheet/CLU058-3618C4_0082P_201710_180423.pdf (reference date: 08.02.2022).
40. Cree Inc. <https://cree-led.com/media/documents/CMU2258.pdf> (reference date: 08.02.22).
41. Cree Inc. <https://cree-led.com/media/documents/ds-CMA2550.pdf> (reference date: 08.02.22).
42. Luo D., Wang L., Or S.W., Zhang H., Xie R.-J. Realizing superior white LEDs with both high R9 and luminous efficacy by using dual red phosphors. *RSC Adv.* 2017. **7**, No 42. P. 25964–25968. <https://doi.org/10.1039/C7RA04614F>.
43. Yao L., He S., Nie W. *et al.* Enhanced red emission from Mn⁴⁺ activated phosphor induced by fluoride to oxyfluoride phase transformation. *J. Lumin.* 2021. **238**. P. 118315. <http://dx.doi.org/10.1016/j.jlumin.2021.118315>.
44. Hong S.C., Ko J.H. Effects of scattering particles on the color rendering and color dispersion of white light-emitting diodes studied by optical simulation. *J. Korean Phys. Soc.* 2021. **79**. P. 631–637. <https://doi.org/10.1007/s40042-021-00285-x>.

45. Smith T., Guild J. The C.I.E. colorimetric standards and their use. *Trans. Opt. Soc.* 1931. **33**, No 3. P. 73–134. <https://doi.org/10.1088/1475-4878/33/3/301>.
46. MacAdam D.L. Projective transformations of I.C.I. color specifications. *JOSA.* 1937. **27**, No 8. P. 294–299. <https://doi.org/10.1364/JOSA.27.000294>.
47. Robertson A.R. Computation of correlated color temperature and distribution temperature. *J. Opt. Soc. Amer.* 1968. **58**. P. 1528–1535. <https://opg.optica.org/josa/abstract.cfm?URI=josa-58-11-1528>.
48. McCamy C.S. Correlated color temperature as an explicit function of chromaticity coordinates. *Color Research & Application.* 1992. **17**, No 2. P. 142–144. <https://doi.org/10.1002/col.5080170211>.
49. Ohno Y. Practical use and calculation of CCT and Duv. *LEUKOS.* 2014. **10**, No 1. P. 47–55. <https://doi.org/10.1080/15502724.2014.839020>.
50. Smet K.A.G. Tutorial: The LuxPy Python Toolbox for Lighting and Color Science. *LEUKOS.* 2020. **16**, No 3. P. 179–201. <https://doi.org/10.1080/15502724.2018.1518717>.
51. “LED ColorCalculator,” Version 7.15, OSRAM SYLVANIA, Massachusetts, <https://www.osram.us/cb/tools-and-resources/applications/led-colorcalculator/index.jsp>

Authors and CV



Demid V. Pekur, PhD, Deputy Head of Optoelectronics Department at the V. Lashkaryov Institute of Semiconductor Physics, NAS of Ukraine. The author of more than 40 scientific publications. His research interests include the development of advanced high-power lighting systems with LED cooling based

on two-phase heat-transfer devices and creation of lighting systems with a wide range of functions. <https://orcid.org/0000-0002-4342-5717>



Viktor M. Sorokin, Professor, Doctor of Sciences, Corresponding Member of NAS of Ukraine, Principal Researcher of Optoelectronics Department at the V. Lashkaryov Institute of Semiconductor Physics, NAS of Ukraine. The author of more than 200 scientific publications. His research interests

include problems of liquid crystal materials science, lighting engineering and lighting materials. He organized massive implementation of LED lighting in Ukraine. He is the State Prize winner of Ukraine in the field of science and technology. <https://orcid.org/0000-0002-1499-1357>



Yurii E. Nikolaenko, Doctor of Engineering. Leading Fellow of the Heat-and-power Engineering Department at the National Technical University of Ukraine “Igor Sikorsky Kyiv Polytechnic Institute”. He is the author of more than 350 scientific publications.

The main direction of scientific LED activity is devices, photovoltaics, heat exchange and provision of thermal modes of electronic equipment and super-power LED lighting devices with the use of heat pipes.

E-mail: yunikola@ukr.net,
<https://orcid.org/0000-0002-3036-5305>



Iлона V. Pekur, lead engineer of the Department of Optoelectronics at the V. Lashkaryov Institute of Semiconductor Physics, NAS of Ukraine. Her research interests include architectural and design challenges in the fields of lighting urbanism, luminaire design and lighting system design.

E-mail: ilona.pekur@gmail.com,
<https://orcid.org/0000-0001-5517-7805>



Margarita A. Minyaylo, researcher at the V. Lashkaryov Institute of Semiconductor Physics, NAS of Ukraine, author of more than 40 publications in scientific journals and 6 patents for inventions. Her scientific works are devoted to investigations of properties of organic light-emitting

structures, photometric and electrical parameters of LEDs and lighting systems of various types, as well as physical-technological and metrological aspects of creating modern lighting systems.

E-mail: margarita.miniailo@gmail.com,
<https://orcid.org/0000-0003-4915-8143>

Authors' contributions

Pekur D.V.: writing – original draft, investigation, data curation, visualization.

Sorokin V.M.: conceptualization, funding acquisition, methodology, supervision, project administration.

Nikolaenko Yu.E.: conceptualization, writing – review & editing.

Pekur I.V.: writing – review & editing, validation, resources, formal analysis, investigation.

Minyaylo M.A.: writing – review & editing, investigation.

Визначення оптичних параметрів квазімонохроматичних світлодіодів для створення систем освітлення з регульованою корельованою колірною температурою

Д.В. Пекур, В.М. Сорокін, Ю.Є. Ніколаєнко, І.В. Пекур, М.А. Міняйло

Анотація. У статті запропоновано новий спосіб визначення оптимальних пікових довжин хвиль квазімонохроматичних світлодіодів при комбінуванні їх з широкосмуговими потужними білими світлодіодами для систем освітлення з регульованою корельованою колірною температурою. На основі моделювання спектра результуючого випромінювання показано придатність розробленого способу для реалізації світлодіодних систем освітлення з можливістю зміни параметрів синтезованого світла. Визначено довжини хвиль квазімонохроматичних світлодіодів (474 та 600 нм), які забезпечують найбільш широкий діапазон регулювання корельованої колірної температури в комбінації з базовим білим світлодіодом (CreeCMA 2550). Квазімонохроматичні світлодіоди з визначеними оптимальними спектральними параметрами дозволяють забезпечити регулювання корельованої колірної температури в діапазоні від 3098 до 6712 К при підтримці високих значень індексу кольоропередачі (понад 80) на переважній (від 3098 до 5600 К) частині доступного діапазону регулювання.

Ключові слова: світлодіод, регульоване біле світло, штучне освітлення, корельована колірна температура, Duv, індекс кольоропередачі.